Ryanodine receptor 2 inhibition reduces dispersion of cardiac repolarization, improves contractile function and prevents sudden arrhythmic death in failing hearts

Pooja Joshi [1], Shanea Estes [1], Deeptankar DeMazumder [2,3,4], Bjorn C. Knollmann [1], Swati Dey [1]*

1. Division of Clinical Pharmacology, Department of Medicine, Vanderbilt University Medical Center, Nashville, Tennessee.
2. Indiana Institute for Medical Research, Veterans Administration Medical Center, Indianapolis, Indiana.
3. Section of Cardiac Electrophysiology, Division of Cardiology, Department of Internal Medicine, University of Pittsburgh Medical Center, Pittsburgh, Pennsylvania.
4. McGowan Institute for Regenerative Medicine, Department of Surgery, University of Pittsburgh School of Medicine, Pittsburgh, Pennsylvania.

*** Correspondence to:**
Swati Dey, PhD
Division of Clinical Pharmacology
Department of Medicine
Vanderbilt University Medical Center
2215B Garland Avenue
Nashville, Tennessee
swati.dey@vumc.org

Abstract

Introduction: Sudden cardiac death (SCD) from ventricular tachycardia/fibrillation (VT/VF) are a leading cause of death, but current therapies are limited. Despite extensive research on drugs targeting sarcolemmal ion channels, none have proven sufficiently effective for preventing SCD. Sarcoplasmic ryanodine receptor 2 (RyR2) Ca^{2+} release channels, the downstream effectors of sarcolemmal ion channels, are underexplored in this context. Recent evidence implicates reactive oxygen species (ROS)-mediated oxidation and hyperactivity of RyR2s in the pathophysiology of SCD.

Objective: To test the hypothesis that RyR2 inhibition of failing arrhythmogenic hearts reduces sarcoplasmic Ca^{2+} leak and repolarization lability, mitigates VT/VF/SCD and improves contractile function.

Methods: We used a guinea pig model that replicates key clinical aspects of human nonischemic HF, such as a prolonged QT interval, a high prevalence of spontaneous arrhythmic SCD, and profound Ca^{2+} leak via a hyperactive RyR2. HF animals were randomized to receive dantrolene (DS) or placebo in early or chronic HF. We assessed the incidence of VT/VF and SCD (primary outcome), ECG heart rate and QT variability, echocardiographic left ventricular (LV) structure and function, immunohistochemical LV fibrosis, and sarcoplasmic RyR2 oxidation.

Results: DS treatment prevented VT/VF and SCD by decreasing dispersion of repolarization and ventricular arrhythmias. Compared to placebo, DS lowered resting heart rate, preserved chronotropic competency during transient β-adrenergic challenge, and improved heart rate variability and cardiac function.

Conclusion: Inhibition of RyR2 hyperactivity with dantrolene mitigates the vicious cycle of sarcoplasmic Ca^{2+} leak-induced increases in diastolic Ca^{2+} and ROS-mediated RyR2 oxidation, thereby increasing repolarization lability and protecting against VT/VF/SCD. Moreover, the consequent increase in sarcoplasmic Ca^{2+} load improves contractile function. These potentially life-saving effects of RyR2 inhibition warrant further investigation, such as clinical studies of repurposing dantrolene as a potential new therapy for heart failure and/or SCD.

Abbreviations

DS	Dantrolene Sodium
EDV	End Diastolic Volume
ESV	End Systolic Volume
FS	Fractional Shortening
HF	Heart Failure
HRV	Heart Rate Variability
ICD	Implantable Cardioverter-Defibrillators
LV	Left Ventricle
PTM	Post-Translational Modifications
ROS	Reactive Oxygen Species
RWT	Relative Wall Thickness
RyR2	Ryanodine Receptor 2
SCD	Sudden Cardiac Death
VT/VF	Ventricular Tachycardia/Ventricular Fibrillation

β-AR β-adrenergic receptors

Introduction

Sudden cardiac death (SCD) in heart failure (HF) is the leading cause of death in the modern world. Current therapies for preventing SCD due to ventricular tachycardia/fibrillation (VT/VF) are limited. For example, implantable cardioverter-defibrillators (ICDs), the only effective therapy for VT/VF and SCD, are palliative, expensive, and pose several risks. Moreover, many patients suffer from VT/VF and SCD in the early stages of HF before they become eligible to receive an ICD[1-9]. Antiarrhythmic drugs, which target ion channels, may confer acute benefits but can also be proarrhythmic, triggering VT/VF. Importantly, most antiarrhythmic drugs worsen survival over the longer term[10,11]. Thus, there is a pressing need to identify new antiarrhythmic targets and develop new therapies for SCD.

A growing body of evidence indicates that sympathetic stress-induced hyperactivity of the ryanodine receptor 2 (RyR2), located in the sarcoplasmic reticulum (SR) of cardiac myocytes, causes SR Ca^{2+} leak, which contributes to the pathogenesis of VT/VF and SCD[12-15]. During systole, the release of Ca^{2+} by the RyR2 plays a pivotal role in myocyte excitation-contraction coupling. The degree of contractility is determined by the amount of Ca^{2+} in the SR and by the timing and magnitude of Ca^{2+} release. In diseased and/or stressed hearts, protein kinase A (PKA)-mediated hyper-phosphorylation and reactive oxygen species (ROS)-mediated oxidation results in a leaky RyR2[10,11], which allows Ca^{2+} to leak out of SR during diastole. The consequent reduction in SR Ca^{2+} load weakens systolic contraction. The consequent rise in cytosolic Ca^{2+} levels also leads to delayed afterdepolarizations (DADs), which can trigger atrial and ventricular tachyarrhythmias[16-19]. Recent evidence suggests that dantrolene, a RyR2 inhibitor, reduces the inducibility of atrial fibrillation in animals with myocardial infarction[20-23]. The effect of RyR2 inhibition on ventricular arrhythmias and non-ischemic HF has been unexplored.

We hypothesized that RyR2 inhibition of failing arrhythmogenic hearts reduces sarcoplasmic Ca^{2+} leak and repolarization lability, mitigates VT/VF/SCD and improves contractile function. The present study employs a guinea-pig model that recapitulates key features of human non-ischemic HF including spontaneous episodes of VT/VF resulting in SCD[24-26]. We examine the effects of chronic dantrolene treatment on the incidence of VT/VF and SCD incidence as non-ischemic HF develops and progresses. In cross-over studies, we determine whether RyR2 inhibition reverses HF and SCD risk. The findings have important implications for repurposing dantrolene, a clinically-used RyR2 inhibitor, as a potential new therapy for HF and SCD.

Results

1. Inhibition of RyR2 leak with dantrolene therapy prevents VT/VF and SCD.

To study the effects of RyR2 leak inhibition on SCD and HF, we leveraged the pressure overload guinea pig model of HF/SCD with spontaneous arrhythmias. Unique to this model is the high incidence of premature ventricular contractions (PVCs) and VT/VF, leading to SCD in about two-thirds of the animals within 4 weeks. Notably, the SCD occurs early on, in the first 2 weeks over the course of cardiac hypertrophy, even before the heart dilates or progresses into failure[24,25]. Hence, the primary endpoint of our study was SCD, and the secondary endpoint was cardiac contractility measured by echocardiography at four weeks. To determine if Dantrolene sodium (DS) treatment can be used as a potential therapeutic agent, we treated the HF/SCD animals with and without oral DS in the early stages of heart failure **(Fig. 1A)**. HF animals exhibit frequent PVCs that often trigger sustained and non-sustained VT and VF, causing SCD **(Fig. 1B)**. DS treatment not only drastically reduced the rate of PVCs in early and late stages of HF **(Fig. 1C)**, but also improved survival **(Fig. 1D)**. Compared to the HF group, the HF+DS group had a significantly higher rate of survival (55% HF vs 80% in HF+DS, $p<0.05$).

2. Dantrolene therapy improves cardiac function and prevents HF.

Cardiac structure and function were preserved in HF animal treated with DS as compared to the HF group. In contrast to the HF group, the HF+DS group did not display a significant dilation of the left ventricle (LV) at the 4-week endpoint **(Fig. 2A)**. Echocardiography measures **(Fig. 2B)** show that the

relative wall thickness (RWT), which is a measure of the LV dimensions and is a marker for adverse events in LV dysfunction, was significantly lower in HF group as compared to control **(Fig. 2C,** $p<0.05$**)**. Progressive decline of the RWT causes the end systolic volume (ESV) and the end diastolic volume (EDV) to increase and cardiac output to decrease. Reduced contractility and increased afterload both reduce the ejection fraction and increase end-systolic volumes in failing hearts **(Fig. 2D-F)**. Additionally, EDV increased (not shown) without an increase in the stroke volume. To summarize, chronic DS therapy in HF prevented the thinning of the LV walls and the eventual decline in cardiac contractility.

3. Dantrolene prevents myocardial structural and molecular damage.

Analysis of the myocardial structure showed increase in interstitial fibrosis in the HF group compared to the normal controls. Whereas the fibrotic tissue was twofold higher in the untreated HF group compared to normal hearts, the HF+DS group displayed lower fibrotic tissue thereby confirming that DS therapy was delaying the progression of HF, keeping the myocardial architecture intact **(Fig. 3A-B)**. Interstitial fibrosis is a histological hallmark associated with the progression of HF and can causes lethal arrhythmias due to reentry circuits.

In our previous report, we noted HF-associated changes in both expression and phospho-proteome of key ion channels, transporters, and excitation contraction-coupling proteins. In particular, hyperphosphorylation of several RyR2 sites were noted in failing hearts when compared to normal[24](**Supplementary Fig S1)**. A targeted antioxidant therapy prevented these modifications, pointing to oxidative damage as the primary cause. Therefore, we tested if DS therapy prevented the downstream oxidative damages by quantifying the oxidation profile of RyR2 with and without DS. RyR2 oxidation was significantly reduced in HF+DS group as compared to HF group **(Fig. 3C)**.

4. Dantrolene treatment decreases heart rate and improves chronotropic competency in HF/SCD.

As per our experimental protocol, all groups of animals received a daily low dosage isoproterenol bolus for one hour. As anticipated, the heart rate was elevated in response to β-adrenergic stimulation and recovered to resting heart rate 3-4 hours later. We assessed ECG parameters at resting heart rate and during post β-AR stress recovery **(Fig. 4A)**. As expected, to adequately respond to the metabolic demand and increased workload, failing hearts fine-tune the resting heart rate. The HF animals had a significant elevation of the resting heart rate (269 ± 10 bpm) as compared to normal controls (251 ± 5, $p<0.005$). HF+DS animals, however, demonstrated a significantly lower heart rate compared to the HF group, which was similar to that of normal controls (243 ± 5 bpm, $p<0.005$) **(Fig. 4B)**. Paired analysis of the heart rate for each subject over 4 weeks show that HF animals experienced an increase in resting heart rate by 20-40 bpm. Whereas HF+DS animals experienced a decreased in heart rate by a minimum of 20-30 bpm. The histogram in **Figure 4C** depicts the distribution of heart rate over a 24-hour period from the normal, HF, and HF+DS groups, demonstrating the decreased heart rate in the HF+DS group.

Despite increased resting heart rate, the peak response to transient β-AR stress was much lower in HF than HF+DS group, indicative of the therapeutic role of DS in restoring chronotropic competence in failing hearts. Chronotropic competence describes the capacity of the heart to increase its rate in response to increased demand effectively. The average increase in heart rate during transient stress in HF group (96 ± 5 bpm) was significantly lower ($p<0.05$) than HF+DS group (114 ± 9 bpm). Furthermore, the heart rate variability (HRV, SDNN) was higher in HF+DS group (9.00 ± 0.21) at rest and post stress recovery **(Fig. 4D)**, similar to normal animals as compared to HF (7.28 ± 0.16; $p<0.005$). DS treatment not only restored the chronotropic response to stress but also reduced the incidences of VT/VF and SCD. To understand this protective mechanism, we next tested the hypothesis that DS prevents VT/VF and SCD by preventing repolarization abnormalities.

5. Dantrolene prevents repolarization abnormalities, normalizes the QT variability, and reduces T-wave heterogeneity.

Detailed analysis of the ECG features revealed how inhibition of the RyR2 leak with DS prevents VT/VF and SCD. QT variability and prolongation are known to have prognostic significance in failing hearts. While prolonged QTc is considered a risk factor for arrhythmias, QT heterogeneity as an add-on

is a surrogate for lethal VT/VF[27]. The HF group displayed prolonged QTc, increased QT variability and repolarization abnormalities **(Fig. 5A)**. The guinea pig model of HF exhibits prolonged QTc, as shown in our previous studies[24,25]. The QTc of HF+DS group was significantly shorter than HF group and was similar to normal animals at resting heart rate (HF vs HF+DS;175.59 ± 4 vs 155.07 ± 10 msec, $p<0.05$). DS treatment not only prevented QTc prolongation **(Fig. 5B)**, but also significantly reduced QT variability. **Figure 5A** also illustrates the temporal dispersion of repolarization by superimposing T waves from a 24-hour period of ECG recording at week four. QT dispersion was reduced in the DS-treated group, thereby imparting greater electrical stability to the heart. The QT variability at resting heart rate and post stress recovery are lower in DS treated HF animals **(Fig. 5C-D)** (HF vs HF+DS; -0.35 ± 0.02 vs -0.58 ± 0.02, $p<0.001$). Inhibiting RyR2 with DS reduced the dispersion of repolarization/QT variability, demonstrating a central role of diastolic calcium in increasing cardiac repolarization lability, and terminating triggered activity.

6. Crossover studies. Dantrolene after HF development mitigates VT/VF and prevent SCD.

A crossover study was designed where (i) only vehicle was administered until the endpoint i.e., week 4 (HF) (ii) DS was administered at the onset of aortic constriction until chronic contractile dysfunction is evident in the HF group (usually 3 weeks post banding; HF+/-DS) or (iii) after HF had already developed (3 weeks post banding; HF-/+DS group) **(Fig. 6A).** HF animals were randomized and were either treated with DS after chronic HF had developed or at the time of aortic banding. In the HF+/-DS group, none of the animals experienced SCD, including the period when DS therapy was stopped **(Fig. 6B)**. Serial echocardiography shows that the FS% in the HF group declines over a period of 4 weeks. DS prevented decline in cardiac function. Interestingly, HF+/-DS group, the fractional shortening does not decline significantly after stopping DS therapy. This could possibly be an effect of the washout period (**Fig. 6C** FS; pre vs post: 43.35 ± 0.45 vs 53.10 ± 3.16, p: ns). In contrast, the HF-/+DS groups experienced SCD similar to that of HF before DS therapy was started. However, after crossover to DS treatment, no further SCD occurred. Notably, HF-/+DS group, which showed poor cardiac function at week 3 was noted to quickly recover and normalize FS% **(Fig. 6C**, FS%; pre vs post: 32.43 ± 3.48 vs 43.10 ± 0.87).

We next examined the ECG parameters **(Fig. 6E-F)** in HF-/+DS group at week 1 (post banding, initial stages of HF), Week 3 (chronic HF) and Week 4 (after starting DS therapy). PVC burden significantly increases in the HF-/+DS group pre-DS therapy but declines sharply post therapy. We observed the opposite effect in the HF+/-DS group, where PVC burden increases after DS therapy is stopped (**Supplementary Fig. S2**). The resting heart rate during chronic HF is significantly higher than pre-HF. After starting DS therapy in chronic failing hearts, we observed a decrease in resting HR to pre-HF levels. Similar trends were seen in the post stress recovery period. Similarly, HRV improved significantly after the start of DS. The QTc interval was shortened after DS treatment as compared to during pre or chronic HF. The QT variability was also reduced after starting DS. Taken together, RyR2 inhibition with DS is effective both in early and late stages of HF, preventing VT/VF and SCD and improving cardiac contractile function.

Discussion

The novel findings of this study are: (1) Inhibition of RyR2 hyperactivity with DS abolishes VT/VF and SCD by normalizing repolarization abnormalities, QTc variability and shortening prolonged QTc in non-ischemic HF; (2) dantrolene improves β-adrenergic signaling and chronotropic competency, thereby improving LV contractility; and (3) inhibition of RyR2 with DS not only prevents the progression of HF but also reverses chronic heart failure. These findings support the idea that the coupling between chronic sympathetic activity and oxidative stress makes RyR2 hyperactive. ROS increases the channel activity by decreasing the threshold for store overload-induced Ca^{2+} release [28-30]. This causes dispersion of calcium transients, reduces repolarization lability leading to spontaneous ectopic beats and VT/VF/SCD in HF[31,32].

Oxidative stress has been centrally implicated in HF. We and others have shown that the ROS dynamics affect the functioning of RyR2[30,33-36]. Increased energy demand and workload due to impaired contractile function and downregulation of antioxidant enzymes lead to high ROS accumulation[37]. This is

followed by an increase in use and shortage of reducing equivalents like NADPH/NADH, that further weakens the antioxidant defense[24,37]. Our previous studies have confirmed that targeting mROS in failing hearts prevents ventricular fibrillation (VT/VF) and sudden cardiac death (SCD), and reverses heart failure. We see that mROS brings about several changes in protein function including oxidation[34], phosphorylation[14,38-41], S-nitrosylation[33,36,42], and remodeling of the contractile machinery. Notably, the RyRs are in proximity to and tightly coupled with the mitochondrial network. They are readily modified by ROS[43-46], via direct oxidation of thiol groups of cysteine residues[44-46] as well as ROS-mediated calcium-independent activation of CaMKII[47], increasing SR calcium leak[48-51] to promote VT[52], and increasing the channel activity by decreasing the threshold for store overload-induced Ca^{2+} release [28-30].

In normal physiology, transient stimulation of the β-adrenergic receptors prompts a positive inotropic response to meet the physiological demands. This includes opening of L-type calcium channels (LTCCs) and the release of cytosolic calcium from the SR, triggering contraction through the activation of ryanodine receptors. Tight regulation of Ca^{2+} release from and reuptake into the sarcoplasmic reticulum is required for proper excitation-contraction coupling. However, in pathology, chronic activation of β-adrenergic receptors is maladaptive, increases ROS which remodels ion channels, modifies proteins, and worsens Ca^{2+} leak from ryanodine receptors; these factors result in EADs or DADs that depose the heart to VT/VF, SCD or injure myocardium; they may also impede contractile machinery. During diastole, the RyR2 still releases a small volume of Ca^{2+} known as the leak. When this leak is continuous, like in failing hearts, the SR Ca^{2+} is depleted and diastolic Ca^{2+} is elevated, which weakens contractile force. At the same time, SR's capacity to retain the Ca^{2+} is compromised. With the efflux of Na via the NCX, the exchanger imports Ca^{2+}, but this influx doesn't not replenish SR Ca^{2+} load, but rather contributes to the diastolic Ca^{2+} [53-56]. The increased Na load also depolarizes membrane potential and reduces conduction velocity, thus increasing anisotropy[57,58]. Additionally, intracellular [Na^{+}] accumulation at higher heart rates decreases Ca^{2+} extrusion by NCX, which may now function in its reverse mode[59,60].

In the GP model of non-ischemic HF and SCD, we found that not only SERCA and RyR2 protein expression was downregulated, but the proteins were also hyperphosphorylated. Treatment with an mROS scavenger prevented these alterations from occurring[24]. Because ROS is a secondary messenger, a systemic antioxidant therapy may suppress cellular signaling. A target like RyR2, which is downstream of ROS and directly involved in Ca^{2+} handling, could be of potential clinical interest. Post-translational modifications by oxidation of the RyR2 during the progression of HF causes leaky RyR2, which decreases SR Ca^{2+} stores and elevated levels of diastolic calcium. Decreased SR Ca^{2+} stores, leads to decreased Ca^{2+} transient amplitude and duration during systole.

Our results show that chronic treatment with dantrolene in HF/SCD animal prevents lethal VT/VF, prevents HF, and delays the onset of cardiac decompensation in pressure overload. The effects of dantrolene on RyR2 were reflected by a decrease in oxidation of the RyR2 at the molecular level, a decrease in PVC burden, and an improvement in survival at the functional level *in vivo*. Pressure overload-induced structural alterations like increased fibrosis[61]. and progressive contractile dysfunction, thinning of ventricular walls and ventricular dilation were successfully ameliorated by chronic dantrolene treatment. Our previous work confirmed that sham controls (sham HF+ isoproterenol challenge in the absence of pressure overload) did not significantly increase fibrosis, although there was a trend towards more[25,26]. Although no mechanistic links between SR calcium leak and fibrosis has been explained, an association between reduced SR Ca^{2+} and fibrosis has been previously reported[34,61,62]. When dantrolene treatment was started after chronic HF was established, the contractile function and electrical properties of the heart started to recover and reverse.

Comprehensive analysis of the electrophysiological properties of the HF/SCD group shows that with chronic HF decrease in heart rate variability, QT prolongation, increase in dispersion of repolarization. An increase in QT variability is due to the reduction of repolarization lability. Reduction of repolarization lability is associated with increased susceptibility of arrhythmogenesis in patients with prolonged QT and/or structural heart disease. With high cytoplasmic Ca^{2+} load, the inward sarcolemmal NCX current might significantly reduce the function of repolarization lability in calcium overloads and induce early (EADs) and delayed after-depolarization (DADs). Subsequently, the vulnerability to arrhythmias is

increased. These local Ca^{2+} handling abnormalities are reflected in beat-to-beat changes in ECG[63] T wave morphology and lability causing augmented QT variability[64,65]. Dantrolene prevents SR Ca^{2+} leak from RyR2 and normalize Ca^{2+}handling, suggesting that SR Ca^{2+} leak is central to Ca^{2+} induced triggered activity. Chronic dantrolene therapy enhanced chronotropic competence in response to increased metabolic demand in addition to correcting ventricular electrophysiological abnormalities, even when DS therapy started after HF had already been established.

Because the electrophysiological, Ca^{2+} handling, autonomic, metabolic, and immune systems of the guinea pig are similar to that of humans, the findings in this study may be more relevant to humans as compared to other small animal models of SCD. For example, the ventricular action potential has a rapid upstroke and long plateau, defined by the balance of inward L-type Ca^{2+} current (Cacna1c) and repolarizing currents carried by the inward rectifier K channel (Kcnj2), and the rapid (Kcnh2) and slow (Kcnq1/Kcne1) components of the delayed rectifier K current, as well as the long cellular action potential plateau morphology that contributes to the prolonged QT interval of human heart failure. Excitation-contraction (EC) coupling displays a 60:35 balance between SR Ca^{2+} reuptake and Na/ Ca^{2+} exchange for Ca^{2+} removal on each beat, as well as a 3:1 β to α myosin heavy chain isoform ratio[66,67]. These properties are remarkably similar to the adult human heart and essential for studying how cardiac remodeling contributes to contractile dysfunction and VT/VF as HF develops and progresses.

Conclusion and future directions

Damage caused by oxidative stress alters the proteomic profile of the cell, including altering expression levels as well as the structure and function of EC-coupling proteins. This study demonstrates that inhibition of Ca^{2+} leak via RyR2 pauses the transition to heart failure by reducing cardiac fibrosis, increasing repolarization lability, and decreasing QT heterogeneity, improving chronotropic competency, ultimately improving LV contractility, and mitigating lethal VT/VF. Given that dantrolene is available for clinical use, future studies should evaluate its efficacy in humans with heart failure.

Footnotes

Author contributions

BCK and SD jointly conceived and designed this study. PJ and SE performed the experiments. SD, DD and PJ performed data analyses and interpreted the results. The manuscript has been read, revised, and approved by all authors.

Sources of funding

This work was supported by American Heart Association Grants AHA19TPA34850151(to SD) and AHA19SFRN34830019 (to BCK), NHLBI/National Institutes of Health Grants NIH 4R00HK130662 (to DD), NIH DP2HL157941 (to DD) and Department of Defense Grants DOD-W81XWH-19-1-0640 (to SD), DOD-W81XWH-20-1-0701 (to SD and DD).

References

1. Aziz, H.*, et al.* Bilateral Cardiac Sympathectomy and Extrapericardial Coil Implantation for the Management of Electrical Storm. *JACC. Case reports* **3**, 491-495 (2021).
2. Butrous, G.S., Gough, W.B., Restivo, M., Yang, H. & el-Sherif, N. Adrenergic effects on reentrant ventricular rhythms in subacute myocardial infarction. *Circulation* **86**, 247-254 (1992).
3. Krishnan, A.*, et al.* Sympathectomy for Stabilization of Heart Failure Due to Drug-Refractory Ventricular Tachycardia. *Ann Thorac Surg* **105**, e51-e53 (2018).
4. Richardson, T.*, et al.* Cardiac sympathectomy for the management of ventricular arrhythmias refractory to catheter ablation. *Heart rhythm* **15**, 56-62 (2018).
5. Vaseghi, M.*, et al.* Cardiac Sympathetic Denervation for Refractory Ventricular Arrhythmias. *J Am Coll Cardiol* **69**, 3070-3080 (2017).
6. Yalin, K.*, et al.* Cardiac sympathetic denervation in patients with nonischemic cardiomyopathy and refractory ventricular arrhythmias: a single-center experience. *Clinical Research in Cardiology* (2020).
7. Zhou, M.*, et al.* Cardiac Sympathetic Afferent Denervation Protects Against Ventricular Arrhythmias by Modulating Cardiac Sympathetic Nerve Activity During Acute Myocardial Infarction. *Med Sci Monit* **25**, 1984-1993 (2019).
8. Zanoni, F.L.*, et al.* Bilateral sympathectomy improves postinfarction left ventricular remodeling and function. *J Thorac Cardiovasc Surg* **153**, 855-863 (2017).
9. Tygesen, H.*, et al.* Long-term effect of endoscopic transthoracic sympathicotomy on heart rate variability and QT dispersion in severe angina pectoris. *Int J Cardiol* **70**, 283-292 (1999).
10. Echt, D.S.*, et al.* Mortality and morbidity in patients receiving encainide, flecainide, or placebo. The Cardiac Arrhythmia Suppression Trial. *N Engl J Med* **324**, 781-788 (1991).
11. Cardiac Arrhythmia Suppression Trial, I.I.I. Effect of the antiarrhythmic agent moricizine on survival after myocardial infarction. *N Engl J Med* **327**, 227-233 (1992).
12. Fischer, T.H., Maier, L.S. & Sossalla, S. The ryanodine receptor leak: how a tattered receptor plunges the failing heart into crisis. *Heart Fail Rev* **18**, 475-483 (2013).
13. Alvarado, F.J. & Valdivia, H.H. Mechanisms of ryanodine receptor 2 dysfunction in heart failure. *Nat Rev Cardiol* **17**, 748 (2020).
14. Wehrens, X.H.*, et al.* Ryanodine receptor/calcium release channel PKA phosphorylation: a critical mediator of heart failure progression. *Proc Natl Acad Sci U S A* **103**, 511-518 (2006).
15. Eisner, D.A., Kashimura, T., O'Neill, S.C., Venetucci, L.A. & Trafford, A.W. What role does modulation of the ryanodine receptor play in cardiac inotropy and arrhythmogenesis? *J Mol Cell Cardiol* **46**, 474-481 (2009).
16. Al-Khatib, S.M.*, et al.* 2017 AHA/ACC/HRS Guideline for Management of Patients With Ventricular Arrhythmias and the Prevention of Sudden Cardiac Death: A Report of the American College of Cardiology/American Heart Association Task Force on Clinical Practice Guidelines and the Heart Rhythm Society. *Circulation* **138**, e272-e391 (2018).
17. Wehrens, X.H.T. Leaky ryanodine receptors cause delayed afterdepolarizations and ventricular arrhythmiasThe opinions expressed in this article are not necessarily those of the Editors of the European Heart Journal or of the European Society Cardiology. *European Heart Journal* **28**, 1054-1056 (2007).
18. Hamilton, S.*, et al.* Increased RyR2 activity is exacerbated by calcium leak-induced mitochondrial ROS. *Basic Res Cardiol* **115**, 020-0797 (2020).
19. Liu, T.*, et al.* Altered calcium handling produces reentry-promoting action potential alternans in atrial fibrillation-remodeled hearts. *JCI Insight* **5**(2020).
20. Azam, M.A.*, et al.* Cardioprotective effects of dantrolene in doxorubicin-induced cardiomyopathy in mice. *Heart Rhythm O2* **2**, 733-741 (2021).
21. Zamiri, N.*, et al.* Dantrolene improves survival after ventricular fibrillation by mitigating impaired calcium handling in animal models. *Circulation* **129**, 875-885 (2014).

22. Chou, C.C., *et al.* Dantrolene suppresses ventricular ectopy and arrhythmogenicity with acute myocardial infarction in a langendorff-perfused pacing-induced heart failure rabbit model. *J Cardiovasc Electrophysiol* **25**, 431-439 (2014).
23. Meissner, A., Min, J.Y., Haake, N., Hirt, S. & Simon, R. Dantrolene sodium improves the force-frequency relationship and beta-adregenic responsiveness in failing human myocardium. *Eur J Heart Fail* **1**, 177-186 (1999).
24. Dey, S., DeMazumder, D., Sidor, A., Foster, D.B. & O'Rourke, B. Mitochondrial ROS Drive Sudden Cardiac Death and Chronic Proteome Remodeling in Heart Failure. *Circ Res* **123**, 356-371 (2018).
25. Liu, T., *et al.* Inhibiting mitochondrial Na+/Ca2+ exchange prevents sudden death in a Guinea pig model of heart failure. *Circ Res* **115**, 44-54 (2014).
26. Liu, T., Yang, N., Sidor, A. & O'Rourke, B. MCU Overexpression Rescues Inotropy and Reverses Heart Failure by Reducing SR Ca²⁺ Leak. *Circulation Research* **128**, 1191-1204 (2021).
27. Cvijic, M., Antolic, B., Klemen, L. & Zupan, I. Repolarization heterogeneity in patients with cardiac resynchronization therapy and its relation to ventricular tachyarrhythmias. *Heart rhythm* **15**, 1784-1790 (2018).
28. Jiang, D., *et al.* RyR2 mutations linked to ventricular tachycardia and sudden death reduce the threshold for store-overload-induced Ca2+ release (SOICR). *Proc Natl Acad Sci U S A* **101**, 13062-13067 (2004).
29. MacLennan, D.H. & Chen, S.R. Store overload-induced Ca2+ release as a triggering mechanism for CPVT and MH episodes caused by mutations in RYR and CASQ genes. *The Journal of physiology* **587**, 3113-3115 (2009).
30. Waddell, H.M.M., *et al.* Oxidation of RyR2 Has a Biphasic Effect on the Threshold for Store Overload-Induced Calcium Release. *Biophys J* **110**, 2386-2396 (2016).
31. Pogwizd, S.M., McKenzie, J.P. & Cain, M.E. Mechanisms underlying spontaneous and induced ventricular arrhythmias in patients with idiopathic dilated cardiomyopathy. *Circulation* **98**, 2404-2414 (1998).
32. Szabo, B., Kovacs, T. & Lazzara, R. Role of calcium loading in early afterdepolarizations generated by Cs+ in canine and guinea pig Purkinje fibers. *J Cardiovasc Electrophysiol* **6**, 796-812 (1995).
33. Gonzalez, D.R., Treuer, A.V., Castellanos, J., Dulce, R.A. & Hare, J.M. Impaired S-nitrosylation of the ryanodine receptor caused by xanthine oxidase activity contributes to calcium leak in heart failure. *J Biol Chem* **285**, 28938-28945 (2010).
34. Huang, Y., *et al.* Oxidation of Ryanodine Receptors Promotes Ca²⁺ Leakage and Contributes to Right Ventricular Dysfunction in Pulmonary Hypertension. *Hypertension* **77**, 59-71 (2021).
35. Hamilton, S., *et al.* Increased RyR2 activity is exacerbated by calcium leak-induced mitochondrial ROS. *Basic Research in Cardiology* **115**, 38 (2020).
36. Nikolaienko, R., Bovo, E. & Zima, A.V. Redox Dependent Modifications of Ryanodine Receptor: Basic Mechanisms and Implications in Heart Diseases. *Front Physiol* **9**, 1775 (2018).
37. Foster, D.B., *et al.* Integrated Omic Analysis of a Guinea Pig Model of Heart Failure and Sudden Cardiac Death. *J Proteome Res* **15**, 3009-3028 (2016).
38. Dobrev, D. & Wehrens, X.H. Role of RyR2 phosphorylation in heart failure and arrhythmias: Controversies around ryanodine receptor phosphorylation in cardiac disease. *Circ Res* **114**, 1311-1319; discussion 1319 (2014).
39. Shan, J., *et al.* Phosphorylation of the ryanodine receptor mediates the cardiac fight or flight response in mice. *J Clin Invest* **120**, 4388-4398 (2010).
40. Uchinoumi, H., *et al.* Catecholaminergic polymorphic ventricular tachycardia is caused by mutation-linked defective conformational regulation of the ryanodine receptor. *Circ Res* **106**, 1413-1424 (2010).

41. van Oort, R.J., *et al.* Ryanodine receptor phosphorylation by calcium/calmodulin-dependent protein kinase II promotes life-threatening ventricular arrhythmias in mice with heart failure. *Circulation* **122**, 2669-2679 (2010).
42. Gonzalez, D.R., Beigi, F., Treuer, A.V. & Hare, J.M. Deficient ryanodine receptor S-nitrosylation increases sarcoplasmic reticulum calcium leak and arrhythmogenesis in cardiomyocytes. *Proc Natl Acad Sci U S A* **104**, 20612-20617 (2007).
43. Bertero, E. & Maack, C. Calcium Signaling and Reactive Oxygen Species in Mitochondria. *Circ Res* **122**, 1460-1478 (2018).
44. Kourie, J.I. Interaction of reactive oxygen species with ion transport mechanisms. *The American journal of physiology* **275**, C1-24 (1998).
45. Zima, A.V. & Blatter, L.A. Redox regulation of cardiac calcium channels and transporters. *Cardiovascular research* **71**, 310-321 (2006).
46. Terentyev, D., *et al.* Redox modification of ryanodine receptors contributes to sarcoplasmic reticulum Ca2+ leak in chronic heart failure. *Circ Res* **103**, 1466-1472 (2008).
47. Curran, J., *et al.* Nitric oxide-dependent activation of CaMKII increases diastolic sarcoplasmic reticulum calcium release in cardiac myocytes in response to adrenergic stimulation. *PLoS One* **9**, e87495 (2014).
48. Ellison, G.M., *et al.* Acute beta-adrenergic overload produces myocyte damage through calcium leakage from the ryanodine receptor 2 but spares cardiac stem cells. *J Biol Chem* **282**, 11397-11409 (2007).
49. Curran, J., Hinton, M.J., Rios, E., Bers, D.M. & Shannon, T.R. Beta-adrenergic enhancement of sarcoplasmic reticulum calcium leak in cardiac myocytes is mediated by calcium/calmodulin-dependent protein kinase. *Circ Res* **100**, 391-398 (2007).
50. Morimoto, S., *et al.* Protein kinase A-dependent phosphorylation of ryanodine receptors increases Ca2+ leak in mouse heart. *Biochemical and biophysical research communications* **390**, 87-92 (2009).
51. Ogrodnik, J. & Niggli, E. Increased Ca(2+) leak and spatiotemporal coherence of Ca(2+) release in cardiomyocytes during beta-adrenergic stimulation. *The Journal of physiology* **588**, 225-242 (2010).
52. Schlotthauer, K. & Bers, D.M. Sarcoplasmic reticulum Ca(2+) release causes myocyte depolarization. Underlying mechanism and threshold for triggered action potentials. *Circ Res* **87**, 774-780 (2000).
53. Milberg, P., *et al.* Acute inhibition of the Na+/Ca2+ exchanger reduces proarrhythmia in an experimental model of chronic heart failure. *Heart rhythm* **9**, 570-578 (2012).
54. Remme, C.A. & Bezzina, C.R. Genetic modulation of cardiac repolarization reserve. *Heart rhythm* **4**, 608-610 (2007).
55. Valdivia, C.R., *et al.* Increased late sodium current in myocytes from a canine heart failure model and from failing human heart. *Journal of molecular and cellular cardiology* **38**, 475-483 (2005).
56. Takano, M., *et al.* Pathophysiological remodeling of mouse cardiac myocytes expressing dominant negative mutant of neuron restrictive silencing factor. *Circulation Journal* **74**, 2712-2719 (2010).
57. Bridge, J.H., Smolley, J.R. & Spitzer, K.W. The Relationship Between Charge Movements Associated with I Ca and I Na-Ca in Cardiac Myocyte. *Science* **248**, 376-378 (1990).
58. Wier, W.G., Egan, T.M., López-López, J.R. & Balke, C.W. Local control of excitation-contraction coupling in rat heart cells. *The Journal of physiology* **474**, 463-471 (1994).
59. Smith, T.W. Digitalis: mechanisms of action and clinical use. *New England Journal of Medicine* **318**, 358-365 (1988).
60. Langer, G.A. Effects of digitalis on myocardial ionic exchange. *Circulation* **46**, 180-187 (1972).
61. Sedej, S., *et al.* Subclinical Abnormalities in Sarcoplasmic Reticulum Ca²⁺ Release Promote Eccentric Myocardial Remodeling and Pump Failure Death in Response to Pressure Overload. *J Am Coll Cardiol* **63**, 1569-1579 (2014).

62. Nofi, C.*, et al.* Chronic dantrolene treatment attenuates cardiac dysfunction and reduces atrial fibrillation inducibility in a rat myocardial infarction heart failure model. *Heart Rhythm O2* **1**, 126-135 (2020).
63. Shusterman, V., Goldberg, A. & London, B. Upsurge in T-wave alternans and nonalternating repolarization instability precedes spontaneous initiation of ventricular tachyarrhythmias in humans. *Circulation* **113**, 2880-2887 (2006).
64. Rosenbaum, D.S.*, et al.* Electrical alternans and vulnerability to ventricular arrhythmias. *N Engl J Med* **330**, 235-241 (1994).
65. Gold, M.R.*, et al.* Role of microvolt T-wave alternans in assessment of arrhythmia vulnerability among patients with heart failure and systolic dysfunction: primary results from the T-wave alternans sudden cardiac death in heart failure trial substudy. *Circulation* **118**, 2022-2028 (2008).
66. Miyata, S., Minobe, W., Bristow, M.R. & Leinwand, L.A. Myosin heavy chain isoform expression in the failing and nonfailing human heart. *Circulation research* **86**, 386-390 (2000).
67. Griffiths, E.J. Species dependence of mitochondrial calcium transients during excitation–contraction coupling in isolated cardiomyocytes. *Biochemical and biophysical research communications* **263**, 554-559 (1999).
68. Hamilton, S.*, et al.* Increased RyR2 activity is exacerbated by calcium leak-induced mitochondrial ROS. *Basic Res Cardiol* **115**, 38 (2020).

Figure Legends

Figure 1. Dantrolene mitigates VT/VF and prevents SCD in vivo. (**A**) Schematic of experimental design. (**B**) Representative ECG tracings from 24-hour telemetry recordings. Spontaneous incidences of PVCs, VT and VF were suppressed in HF animals with chronic DS treatment. (**C**) DS therapy lowered PVC burden ($p<0.001$) in HF animals (blue). (**D**) Kaplan Meier survival plot shows that over 50% of the animals in the vehicle group (HF, N=68, red) group experienced SCD. Chronic DS treatment (HF + DS, N=10, blue) prevented VT and VF in heart failure models and mitigated SCD in 80% of the heart failure animals ($p<0.05$). A $p<0.05$ was considered significant; two-tailed log-rank analysis was performed on each group for each measure.

Figure 2. Dantrolene improves cardiac function and reverses heart failure. (**A**) The hearts in the vehicle group are enlarged, as shown in representative photos of gross hearts (top) and matching cross-sections (bottom) after 4 weeks. In the HF animals, the LV cavity is bigger, and the LV free wall is thinned. Treatment with DS stops the LV walls from thinning. Chronic DS group hearts were normal in size. **(B)** Representative M-mode echocardiography images from all groups (**C-F**) Echocardiography parameters at 4 weeks. HF animals showed significant ($p<0.005$, N: Control=15, HF=20, HF+DS=8)) loss of cardiac function with decline in fractional shortening and relative wall thickness and increase in stroke volume (SV) and end systolic volume (ESV). DS therapy prevented pressure overload dependent structural remodeling of the heart ($p<0.005$).

Figure 3. Dantrolene reverses tissue damage and oxidation profile of RyR2. (**A**) Representative image of Masson trichrome staining in Ctrl, HF & HF+DS hearts (N=3) showing high fibrotic regions as (**B**) summarized. (**C**) The percent carbonyl content/mg of protein was lower in DS treated heart failure animals, showing reversal of RyR2 oxidation profile with DS therapy in HF animals ($p<0.005$, $N\geq4$). A $p<0.05$ was considered significant; two-tailed log-rank analysis was performed on each group for each measure.

Figure 4. Dantrolene treatment decreases heart rate and improves chronotropic competency in HF. (**A**) Plot shows heart rate derived from 24-hour continuous ECG recordings. The animals were subjected to mild transient β-AR stress for 1 hour. Continuous ECG analysis was performed at the following time points: resting heart rate (pre-stress); transient stress and, post stress recovery (4 hours post stress) (**B**) The box plots summarize HR during the resting and recovery phases. The DS treated group (HF+DS) show a lower heart rate (HR) both at rest and post-stress recovery. The Δ Heart Rate (bpm) indicates the net increase in HR from resting HR to peak HR in response to transient β-AR stress. Failing hearts displayed higher resting HR and blunted chronotropic response to stress ($P<0.02$, $N\geq7$ for all models). (**C**) Histogram shows resting HR distribution for all groups. Resting heart rate in decreased in HF+DS animals. However, the peak heart rates (during stress) are higher in HF+DS compared to HF (N; Ctrl=8, HF=10; HF+DS=7). (**D**) DS increases heart rate variability (HRV) both at rest and during stress ($p<0.05$, $N\geq7$ for all models). A $p<0.05$ was considered significant; two-tailed log-rank analysis was performed on each group for each measure.

Figure 5. Dantrolene mitigates repolarization abnormalities, normalizes the QT variability, and reduces T-wave heterogeneity. (**A**) Representative QT segments recorded over 24 hours from Ctrl, HF and HF+DS shows heterogeneity of T wave repolarization in HF (red), but not in HF+DS (blue) animals. DS mitigates increased dispersion of repolarization in HF animals. (**B**) QTc prolongation in HF animals is significantly shortened by DS treatment ($p<0.005$), both a rest and post-stress recovery. The dispersion of repolarization was quantified by measurement of QT variability. (**C**) Increased QT variability predisposes the heart to VT/VF, which is prevented by DS therapy ($p<0.0001$). (**D**) Kernel density plots show that QT variability index increases during rest, transient stress, and post-stress recovery. QT variability recovers quickly post stress in the DS treated group. A $p<0.05$ was considered significant; two-tailed log-rank analysis was performed on each group for each measure.

Figure 6. Dantrolene after HF development can mitigate VT/VF and prevent SCD. (**A**) Schematic illustrates a randomized 2X2 cross-over experimental design to examine the impact of DS therapy. The protocols were as follows (i) only vehicle administered till the endpoint i.e., week 4 (HF), (ii) DS

administered from the onset of HF till until chronic contractile dysfunction is evident in the untreated control HF group (usually 3 weeks post banding; HF+/-DS), or (iii) DS administered after HF had already developed in the HF group (3 weeks post banding; HF-/+DS group). Echocardiography and ECG recordings were taken at week 2/3/4/5. (**B**) Kaplan Meier survival curve showed that 50% of the HF animals experience SCD. Treatment with DS after HF development (around week 3) prevented additional SCDs and improved survival after starting DS therapy in the HFDS-/+ group (purple). Discontinuation of DS however did not increaser mortality in HF+/-DS group(yellow)**.** (**C**) Serial echocardiography plot shows that DS reversed heart failure in HF-/+DS (purple) animals. The FS% in this group initially declined at a pace similar to HF (red) animals, but it quickly normalized as soon as DS therapy was started. However, in the HF+/-DS (yellow) group when the therapy was stopped, the FS% started showing gradual decline, most likely due to washout effect without additional SCD. (**D**) DS treatment pre or post HF development alters RyR2 oxidation of HF animals ($p<0.05$). Treatment with DS reduced RyR2 oxidation even when therapy was initiated or discontinued after HF development. (**E**) Close examination of the HF-/+DS (purple) group, pre and post DS therapy shows an increase in PVC load with progression of HF. **(G)** The box plots summarize QTc pre-HF (light purple), during chronic HF (medium purple) and after DS therapy was initiated (dark purple). The HF-/+DS group displays all symptoms of HF including prolonged QTc after development of HF (around week 3, medium purple box). After start of therapy (dark purple box), QTc shortened at rest and recovery. A $p<0.05$ was considered significant; two-tailed log-rank analysis was performed on each group for each measure.

Figure 7. Graphical abstract. Stress induced ROS increases Ca^{2+} overload via leaky RyR2 channels causing VT/VF and SCD. External or internal stress releases substantial amounts of ROS in the cardiovascular system. This ROS can alter the oxidation/phosphorylation profiles of several EC coupling proteins including RyR2. The altered RyR2 is leaky causing spontaneous calcium release into the cytosol causing early afterdepolarizations (EADs) and diastolic calcium overload causing delayed afterdepolarizations (DADs). This can ultimately lead to triggered activity and cause ventricular tachyarrhythmias (VT/VF) leading to sudden cardiac death (SCD).

Supplemental Figure

Figure S1. Guinea Pig model of HF/SCD shows a remodeled and hyperactive RyR2. (**A**) Proteomics data show decreased RyR2 protein expression in HF animal hearts compared to sham ($p<0.05$ (LIMMA)). (**B**) Carbonyl content assay performed on LV tissue indicates that RyR2 protein is highly oxidized in animals with HF compared to sham/normal ($p<0.005$). (**C**) Baseline ROS assay indicates increased cellular ROS in HF cardiomyocytes compared to normal/sham cardiomyocytes (*$p<0.005$, $N>10$/group). (**D**) Phosphorylation profile of EC coupling proteins in HF cardiac tissue indicates hyperphosphorylation of RyR2 ($p< 0.05$ (LIMMA)). (**E**) HF cardiomyocytes have higher diastolic calcium than normal or sham ($p<0.005$, $N\geq10$/group for all models). A $p<0.05$ was considered significant; two-tailed log-rank analysis was performed on each group for each measure.

Figure S2. Dantrolene after HF development alleviates HF symptoms. (**A**) In the HFDS+/- (yellow) group, PVC burden decreased with chronic DS treatment and increased after DS treatment was stopped. (**B**) HFDS-/+ (purple) group displays all symptoms of HF including increased HR, **(C)** decreased HRV, and **(D)** increased QT variability at week 3 (HF). After start of therapy (week 4), the HR decreased, HRV increased, and QT variability increased at rest and recovery. (**E**) Paired analysis shows % decrease in resting heart rate (bpm) before and after DS therapy in DS+/- (yellow) and DS-/+ (purple) groups. (**F)** Paired analysis indicates that response to β-adrenergic stimulation is blunted in without therapy phase but recovers once DS therapy starts (purple). Vice versa in observed in DS+/- group (yellow). A $p<0.05$ was considered significant; two-tailed log-rank analysis was performed on each group for each measure.

Methods

Animal model: All animal work followed IACUC-approved protocols at the respective institutions. A pressure overload model of HF and SCD was surgically generated with ascending aortic constriction (AC) and a daily bolus of low dose isoproterenol (2mg/kg/day) for β-adrenergic challenge. The surgical procedure and animal model have been previously described in detail[24]. Briefly, animals were anesthetized with isoflurane then intubated. Ascending AC was accomplished by banding the aorta with a 18 mm diameter ligation clip. Throughout the anesthetic event, animals were continuously monitored for vital signs including ECG, pulse oximetry and temperature. Sham animals received a thoracotomy without aortic banding. Daily isoproterenol bolus was delivered via a programmable iPRECIO® pump (Primetech Corp., Tokyo, Japan) implanted in the peritoneal cavity. Animals were randomized to either vehicle or DS. The DS (25 mg/Kg, Patterson Vet catalog# 07-893-7963) was administered via the drinking water. All animals received an ECG transmitter implant (Data Sciences International) in the abdominal cavity and the leads were secured in a lead II axis arrangement. All devices and surgical equipment were gas sterilized (ethylene oxide) or autoclaved. A small subgroup of animals were subjected to a randomized crossover study. The following treatment group were studied:

1. Normal Control
2. HF (AC + once daily β-adrenergic challenge till end point)
3. HF+DS (HF animals received DS therapy till endpoint)
4. HF+DS (+/-) (HF animals received DS therapy till week 3; DS was stopped after week 3)
5. HF+DS (-/+) (HF animals without DS therapy till week 3; DS therapy was started during week 3 and continued till endpoint)

Personnel involved in data collection and analysis were blinded to the treatment and non-treatment groups. All groups received similar incisions and thus, could not be distinguished based on these interventions. Each animal was assigned a unique computer-generated numeric ID. Only male animals were used for this study because of heterogeneity in phenotype of female animals. The progression of HF in female guinea pigs was delayed and the incidence of VT/VF/SCD was distinct from males. Females and ovariectomized females will be the focus of a follow-up study.

Echocardiography: Echocardiography was performed on conscious animals using a L16-4HE Linear Array transducer (5.4 MHz-13.5 MHz) with a Mindray M9 Vet Ultrasound System in a blinded manner. Long axis views were used to obtain two-dimensionally directed M-mode images. Echocardiography measurements from M-mode images were used to determine fractional shortening, wall thickness, cardiac function, volumes, and ejection fraction of the different treatment groups. Three consecutive cardiac cycles by the leading edge-to-leading edge method were used to obtain the measurements. LV end-diastolic and end- systolic dimensions, and LV end-diastolic posterior wall thickness, were measured from the M-mode images, and left ventricular fractional shortening was calculated by the software.

Electrocardiogram (ECG) analysis: Continuous serial ECG recordings were collected using the Data Sciences International, St. Paul MN, telemetry system. Ponemah software was used for data acquisition. Data was exported to and analyzed in a custom developed MATLAB software (MathWorks, Inc., Natick, MA). ECG tracings were reviewed to quantify PVC, VT/VF burden and to adjudicate if death occurred due to SCD. ECG features were extracted from the recordings using the custom MATLAB algorithms and parameters were compared between the various treatment groups.

RyR2 immunoprecipitation and oxidation assay from guinea pig left ventricle tissue: Snap frozen guinea pig LV tissue was lysed using RIPA lysis buffer (Sigma, cat# R0278), supplemented with phosphatase (Roche, cat# 4906837001) and protease inhibitors (Roche, cat# 4693124001). RyR2 was immunoprecipitated from tissue lysate using anti-RyR2 antibody (Invitrogen Cat# MA3916, 5μL) in 0.5 mL RIPA buffer overnight at 4 °C as previously described [68]. Samples were incubated with Protein A/G

Plus agarose beads (Santa Cruz, cat# sc-2003) for 1 h at 4°C and washed three times with RIPA buffer. To determine the oxidation status of RyR2, the Carbonyl Content Assay Kit (Abcam, cat #ab126287) was used, whereby carbonyl groups of immunoprecipitated RyR2 were derivatized to 2,4 dinitrophenylhydrazone (DNP) by reaction with 2,4 dinitrophenylhydrazine which can be quantified using a spectrophotometer at 375nm.

Masson's Trichrome (MT) staining: Connective and fibrotic tissues are stained blue, nuclei are stained deep brown to black, and the cytoplasm is stained red with MT staining. LV tissue was collected from HF animals with and without DS treatment and fixed in 10% neutral buffered formalin. The samples were sectioned and stained at the Translational Pathology Shared Resource at Vanderbilt University.

Statistical analysis: All animal groups were age and weight matched male and randomized to study groups. We use Stata 17 (Stata Corp LP, College Station, TX) for statistical analyses. The Kolmogorov-Smirnov test was used to evaluate normality of distribution. For normal distributions, continuous variables were compared for 2 groups using unpaired t test and ≥3 groups using ANOVA. Non-parametric tests were used for data not normally distributed. Kaplan-Meier analysis was used to compare survival over time between groups. Bonferroni's correction was applied when a sample had multiple time points/treatment measurements. A p value of 0.05 was considered significant and is denoted with an asterisk (*) in the figures.

FIGURE 1

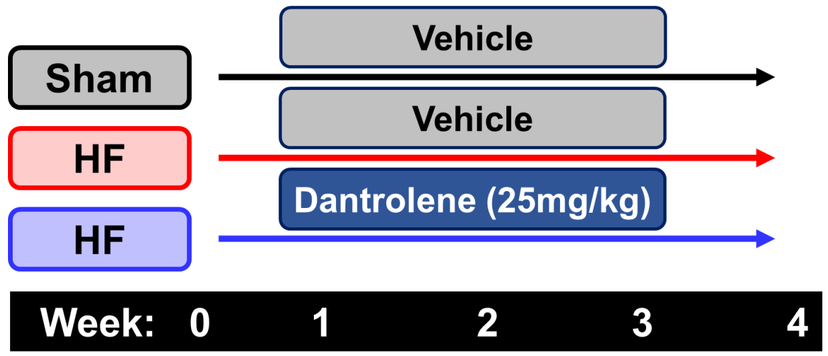
A.
Sham
HF
HF
Vehicle
Vehicle
Dantrolene (25mg/kg)
Week: 0 1 2 3 4

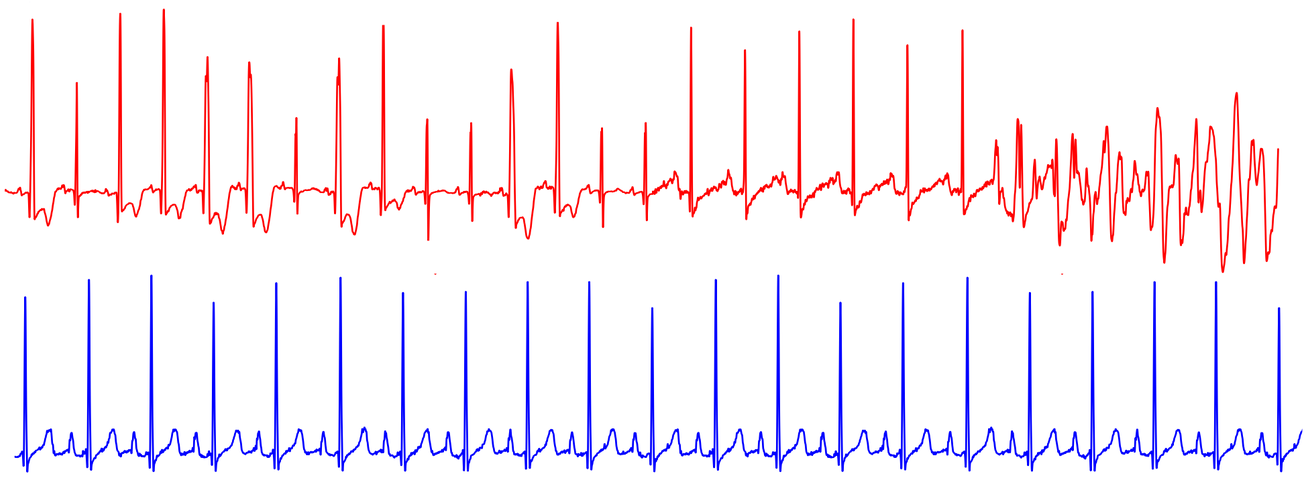
B.

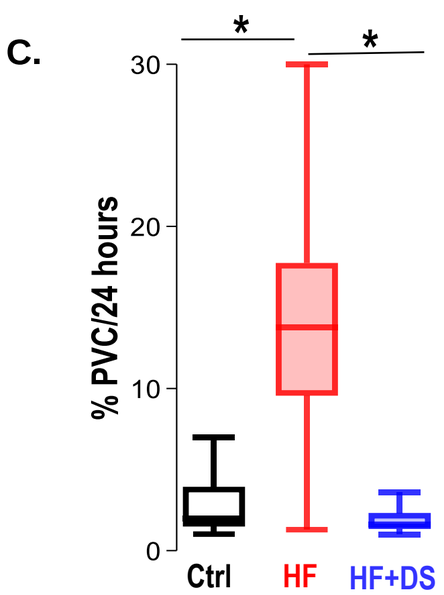
C.
*
*
% PVC/24 hours
30
20
10
0
Ctrl
HF
HF+DS

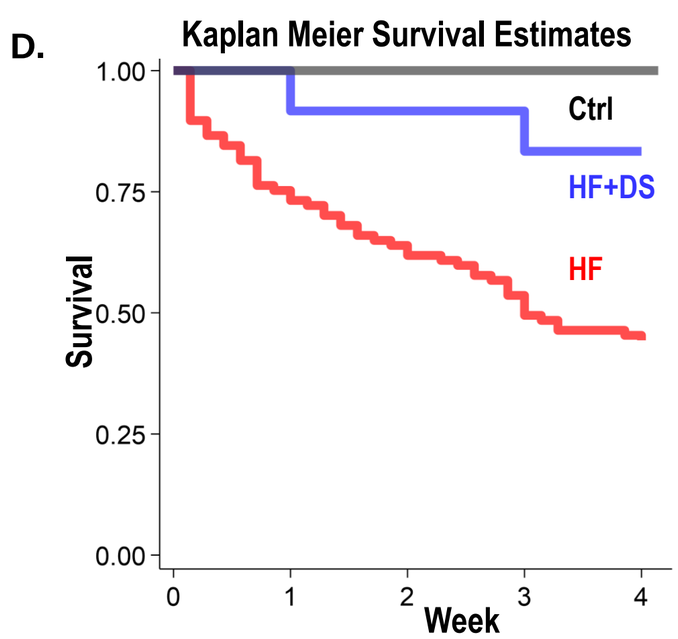
D.
Kaplan Meier Survival Estimates
Survival
1.00
0.75
0.50
0.25
0.00
Ctrl
HF+DS
HF
0
1
2
3
4
Week

FIGURE 2

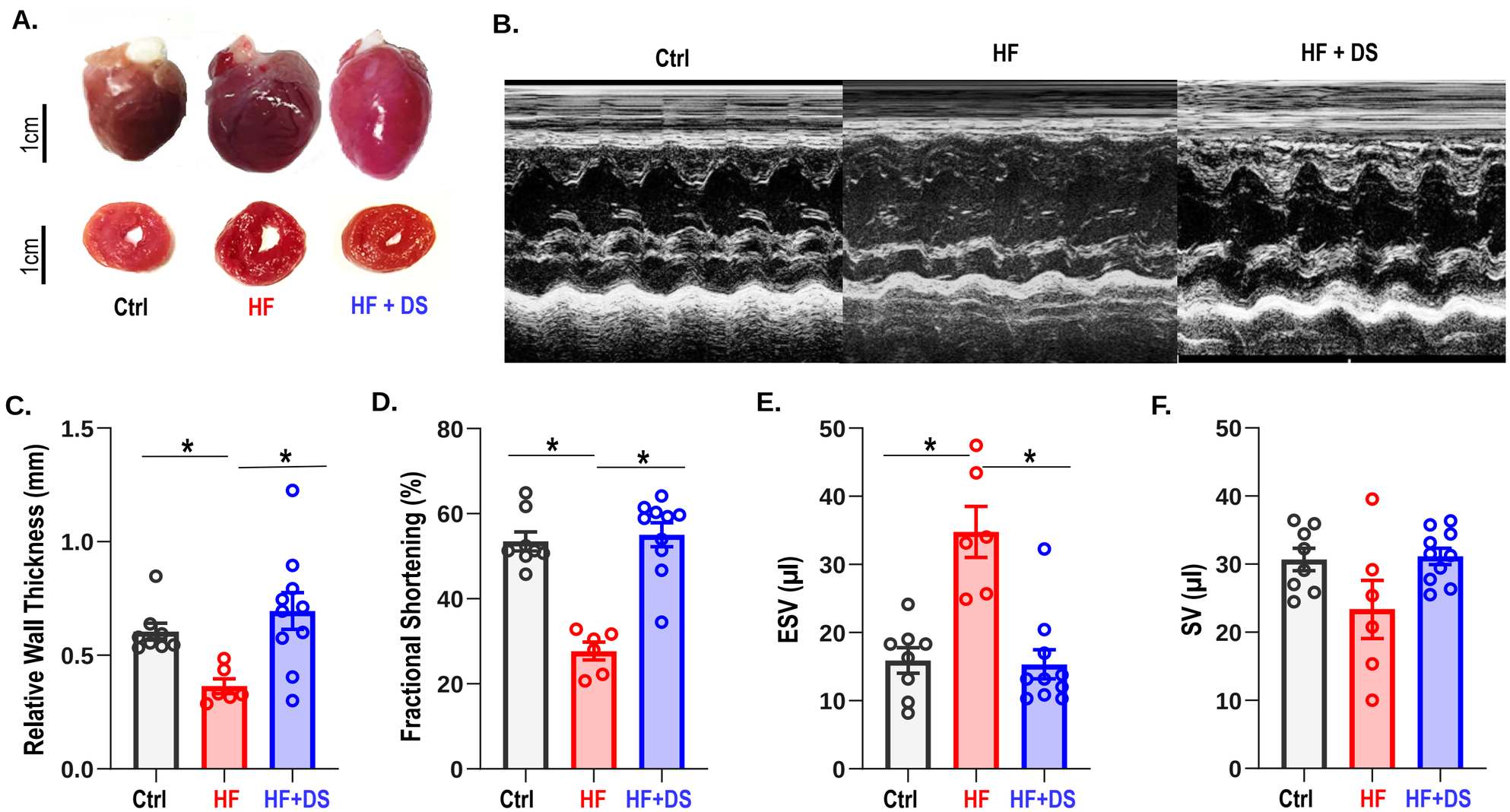
A.
1cm
1cm
Ctrl
HF
HF + DS
B.
Ctrl
HF
HF + DS
C.
Relative Wall Thickness (mm)
1.5
1.0
0.5
0.0
Ctrl
HF
HF+DS
D.
Fractional Shortening (%)
80
60
40
20
0
Ctrl
HF
HF+DS
E.
ESV (µl)
50
40
30
20
10
0
Ctrl
HF
HF+DS
F.
SV (µl)
50
40
30
20
10
0
Ctrl
HF
HF+DS

FIGURE 3

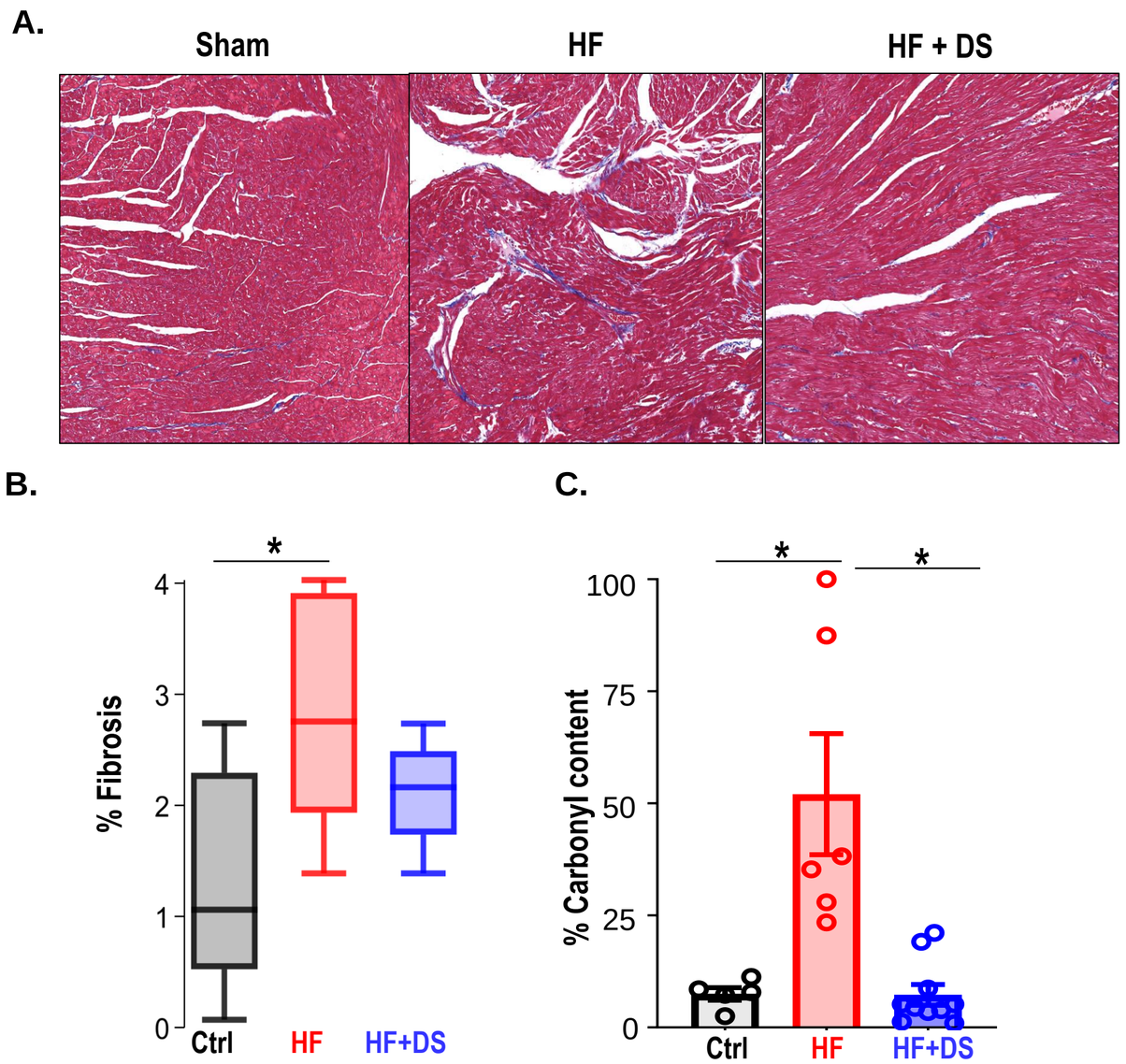
A.
Sham
HF
HF + DS
B.
% Fibrosis
0
1
2
3
4
*
Ctrl
HF
HF+DS
C.
% Carbonyl content
0
25
50
75
100
*
*
Ctrl
HF
HF+DS

FIGURE 4

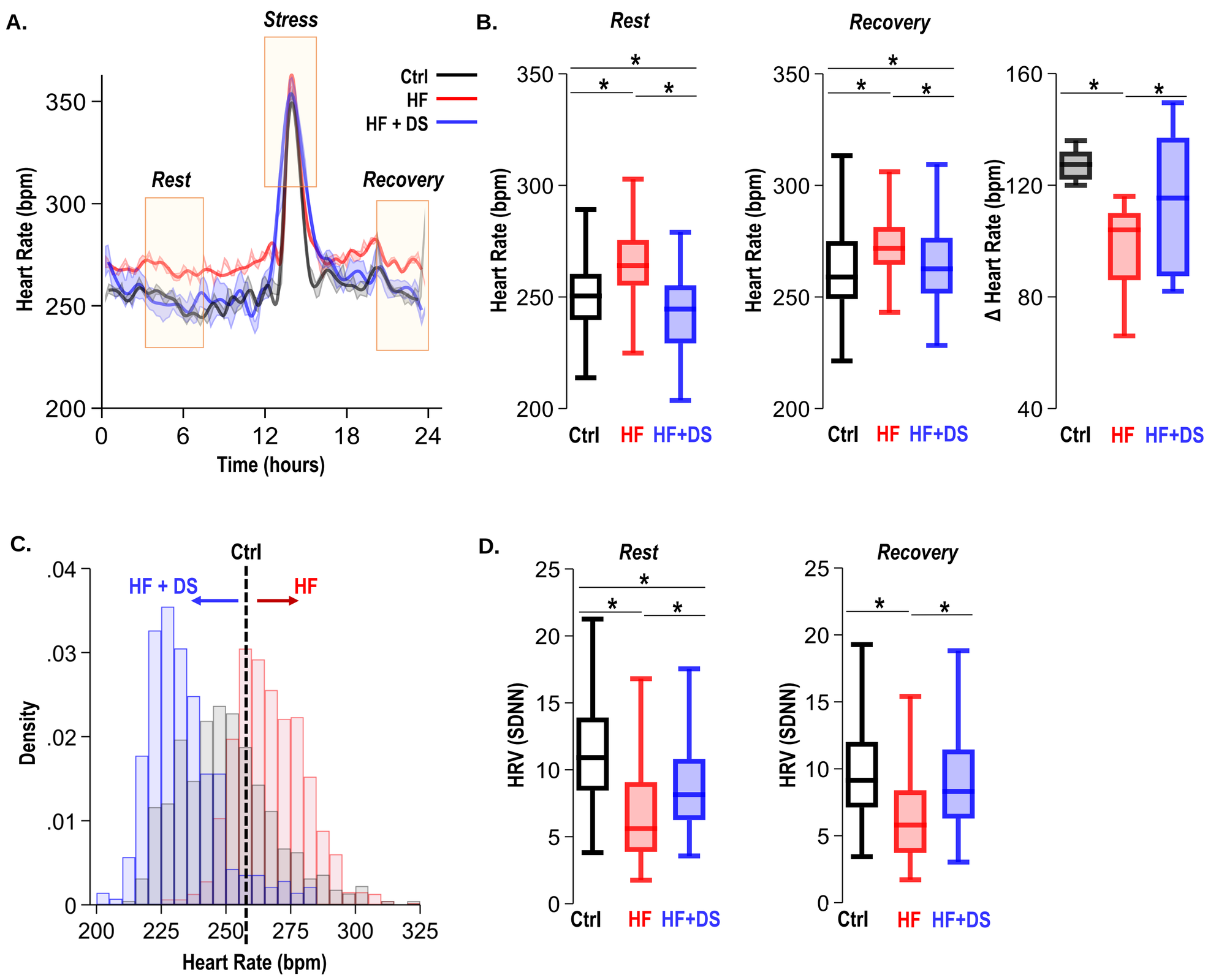
A.
Stress
Rest
Recovery
Ctrl
HF
HF + DS
Heart Rate (bpm)
Time (hours)
B.
Rest
Recovery
Heart Rate (bpm)
Δ Heart Rate (bpm)
Ctrl
HF
HF+DS
C.
Ctrl
HF + DS
HF
Density
Heart Rate (bpm)
D.
Rest
Recovery
HRV (SDNN)
Ctrl
HF
HF+DS

FIGURE 5

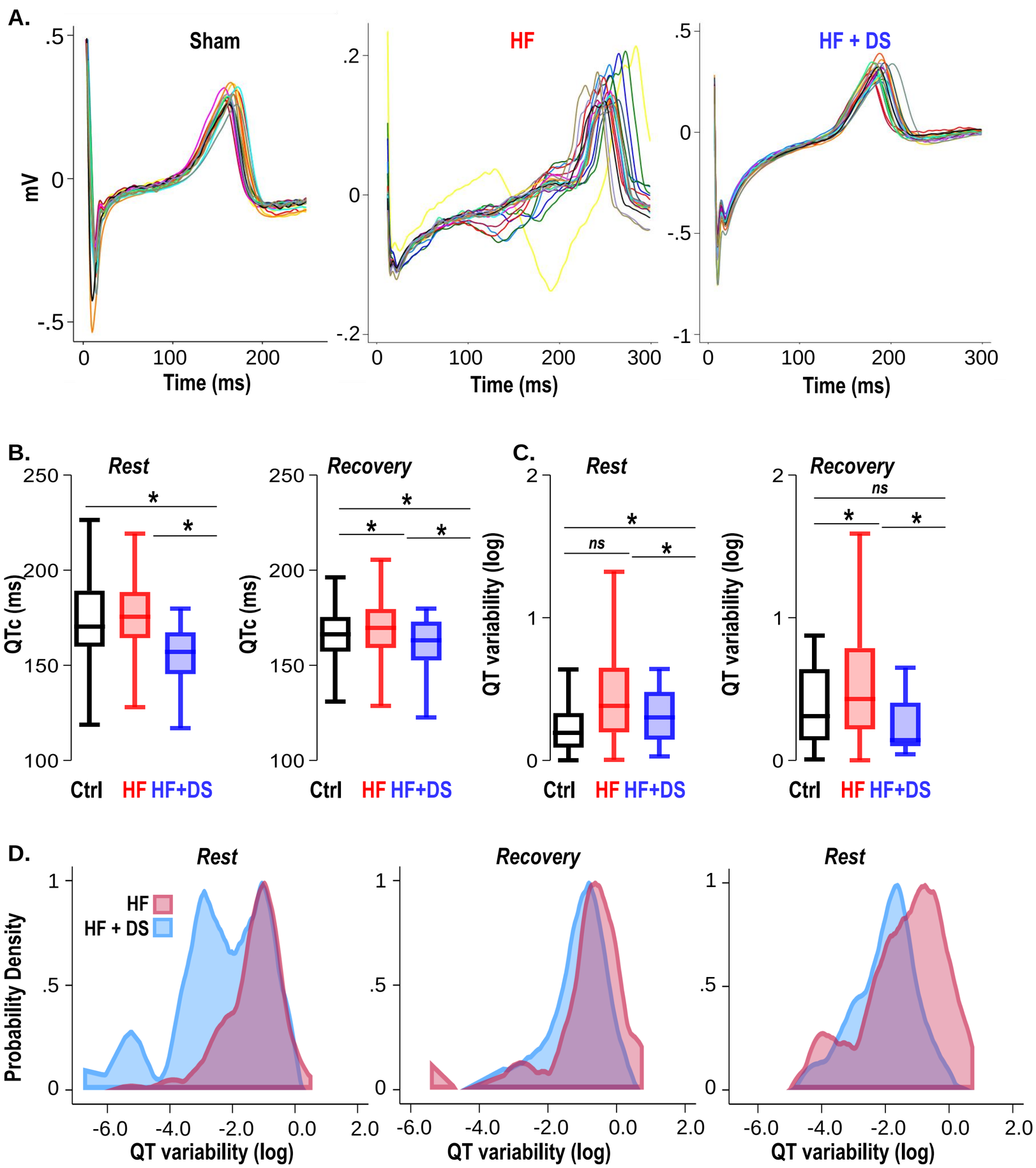
A.
Sham
HF
HF + DS
mV
Time (ms)
B.
Rest
Recovery
QTc (ms)
Ctrl
HF
HF+DS
C.
QT variability (log)
ns
D.
Probability Density
HF
HF + DS
QT variability (log)

FIGURE 6

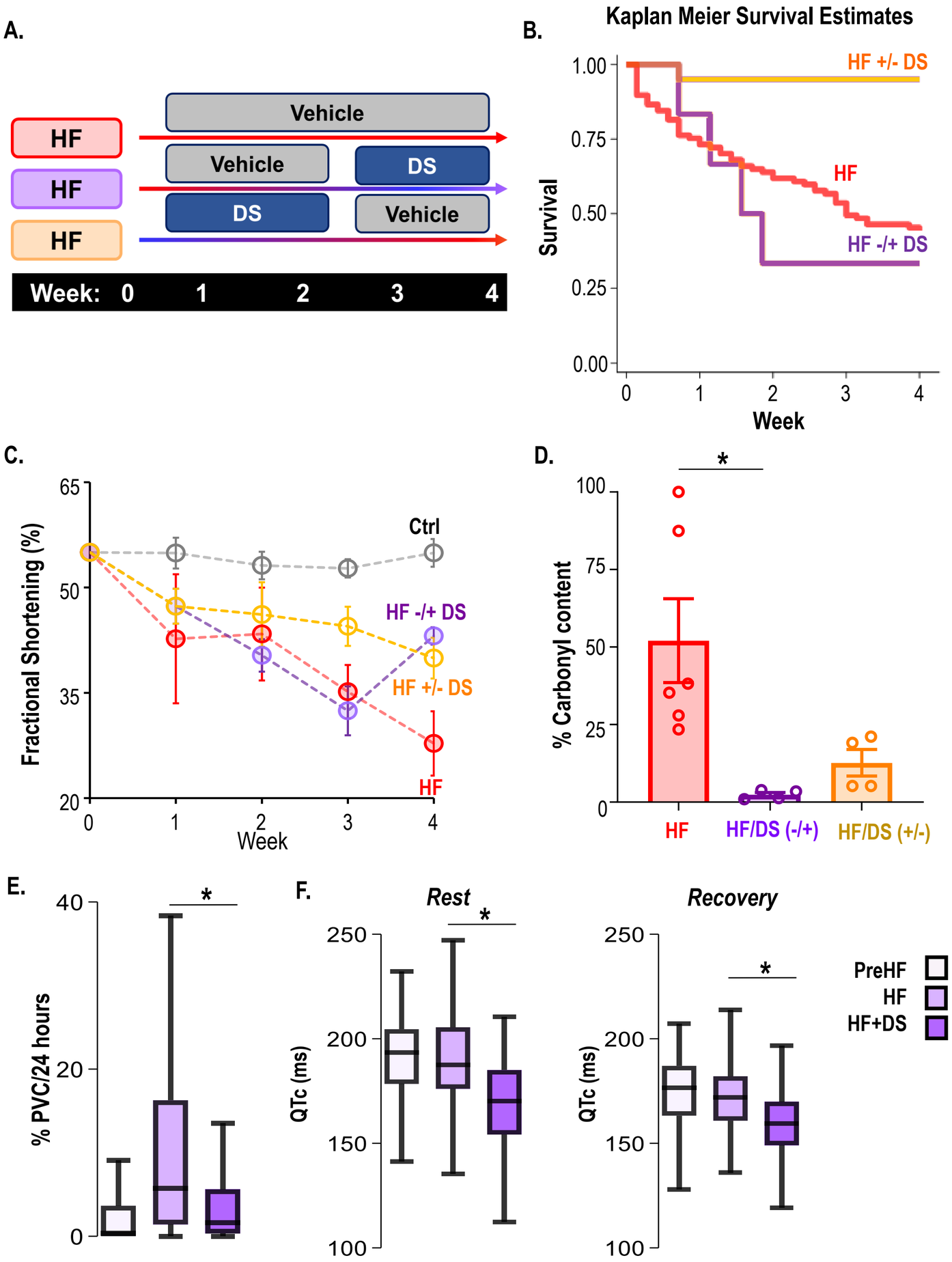
A.
HF
HF
HF
Vehicle
Vehicle
DS
DS
Vehicle
Week: 0 1 2 3 4
B.
Kaplan Meier Survival Estimates
HF +/- DS
HF
HF -/+ DS
Survival
1.00
0.75
0.50
0.25
0.00
0 1 2 3 4
Week
C.
Fractional Shortening (%)
65
50
35
20
Ctrl
HF -/+ DS
HF +/- DS
HF
0 1 2 3 4
Week
D.
% Carbonyl content
100
75
50
25
0
*
HF
HF/DS (-/+)
HF/DS (+/-)
E.
% PVC/24 hours
40
20
0
*
F.
Rest
Recovery
QTc (ms)
250
200
150
100
*
*
PreHF
HF
HF+DS

FIGURE 7

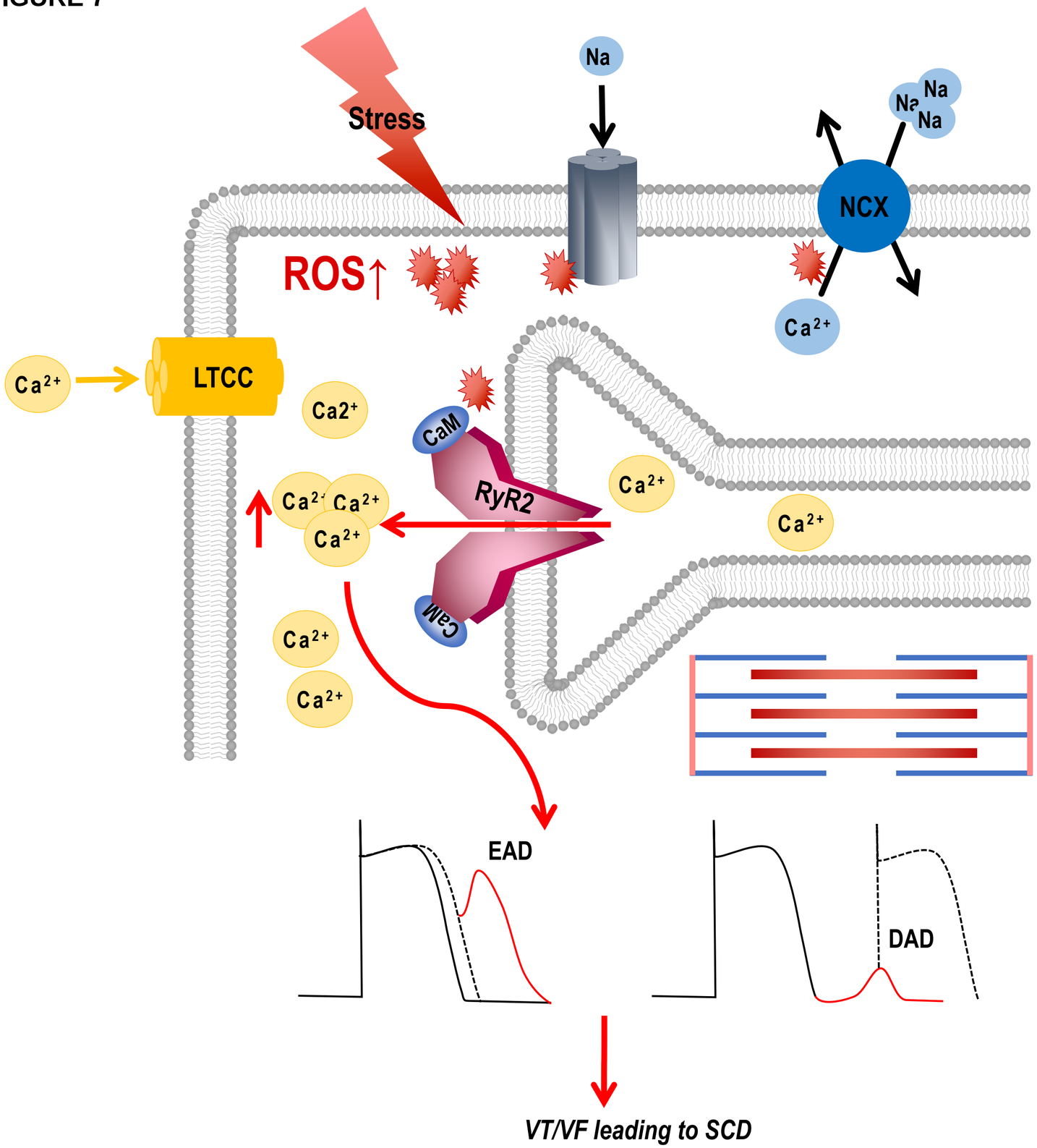
Stress
Na
Na
Na
Na
NCX
ROS↑
Ca2+
Ca2+
LTCC
Ca2+
CaM
RyR2
Ca2+
Ca2+
Ca2+
Ca2+
Ca2+
Ca2+
Ca2+
CaM
Ca2+
Ca2+
EAD
DAD
VT/VF leading to SCD

Figure S1

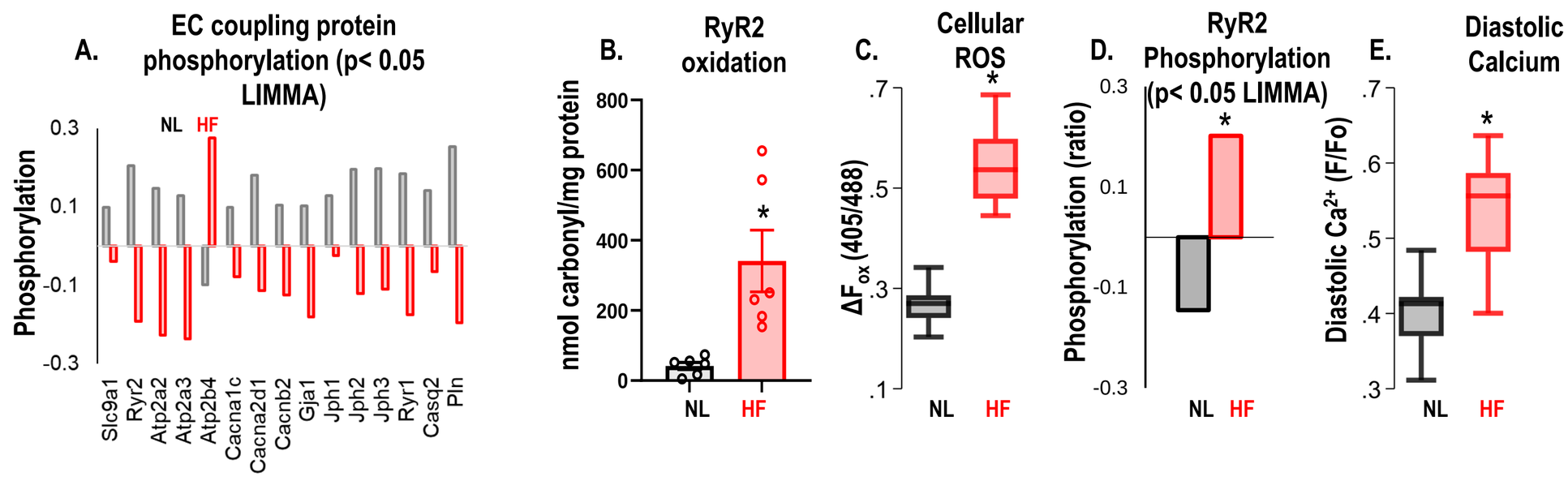
A.
EC coupling protein phosphorylation (p< 0.05 LIMMA)
NL
HF
Phosphorylation
0.3
0.1
-0.1
-0.3
Slc9a1
Ryr2
Atp2a2
Atp2a3
Atp2b4
Cacna1c
Cacna2d1
Cacnb2
Gja1
Jph1
Jph2
Jph3
Ryr1
Casq2
Pln
B.
RyR2 oxidation
nmol carbonyl/mg protein
800
600
400
200
0
*
NL
HF
C.
Cellular ROS
ΔF_ox (405/488)
.7
.5
.3
.1
*
NL
HF
D.
RyR2 Phosphorylation (p< 0.05 LIMMA)
Phosphorylation (ratio)
0.3
0.1
-0.1
-0.3
*
NL
HF
E.
Diastolic Calcium
Diastolic Ca2+ (F/Fo)
.7
.6
.5
.4
.3
*
NL
HF

Figure S2

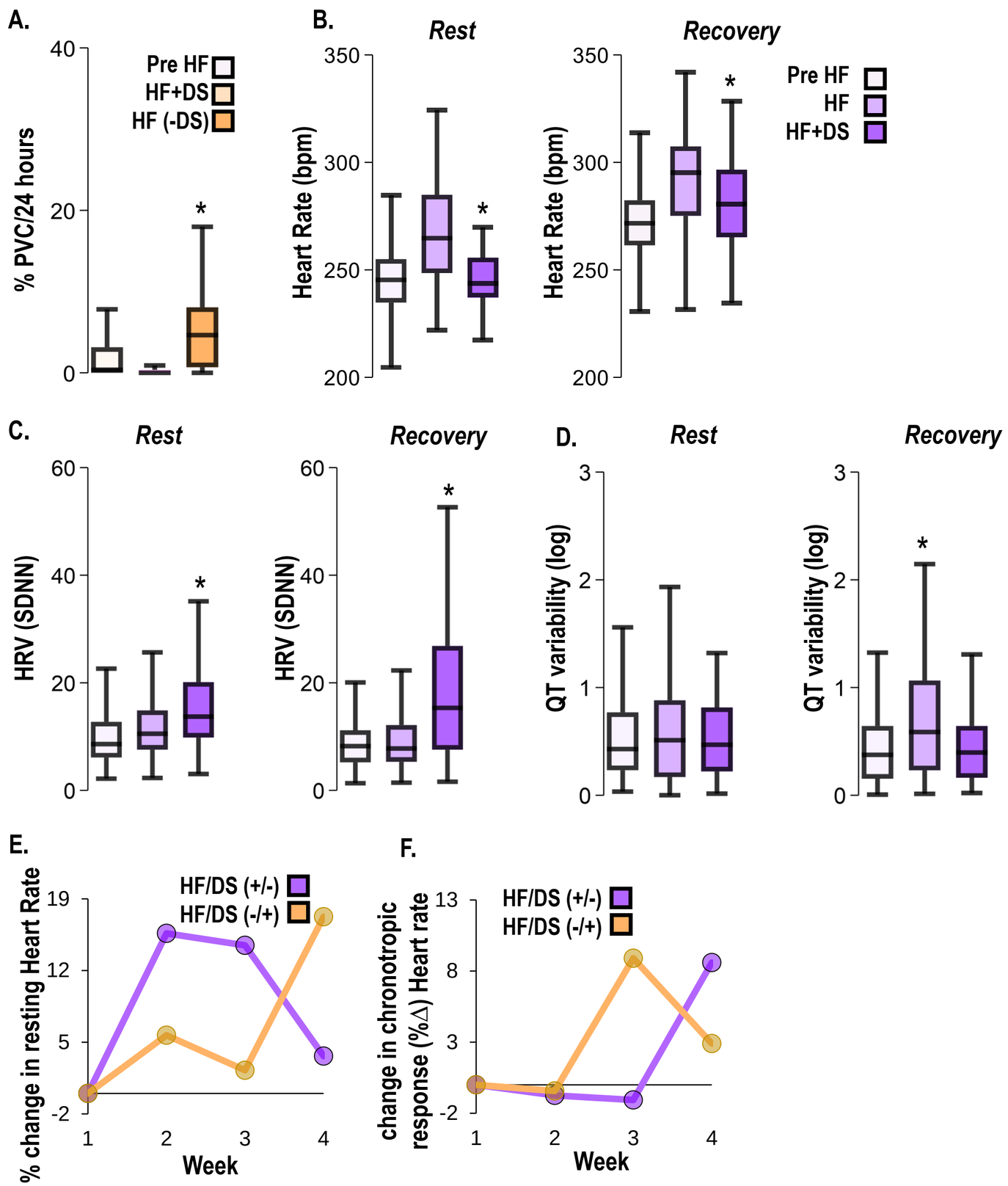
A.
% PVC/24 hours
Pre HF
HF+DS
HF (-DS)
B.
Rest
Recovery
Heart Rate (bpm)
Pre HF
HF
HF+DS
C.
Rest
Recovery
HRV (SDNN)
D.
Rest
Recovery
QT variability (log)
E.
% change in resting Heart Rate
HF/DS (+/-)
HF/DS (-/+)
Week
F.
change in chronotropic response (%Δ) Heart rate
HF/DS (+/-)
HF/DS (-/+)
Week